16TH EUROPEAN CONFERENCE ON EARTHQUAKE ENGINEERING THESSALONIKI 18 - 21 JUNE 2018

REAL APERTURE RADAR. AN INTERFEROMETRIC TECHNIQUE TO ASSESS EARTHQUAKE DAMAGED STRUCTURES

Esteban CABRERA[1], Ramon G. DRIGO[2], Guido LUZI[3], Yeudy VARGAS[4], Luis G. PUJADES[5]

ABSTRACT

Ambient vibration testing has become a useful tool to assess the operational conditions of any existing structure, and allows the engineers to maintain a continuous monitoring in order to check its structural health conditions. In this paper an experimental survey performed by means of an original interferometric technique applied on a real building damaged after the Mw 5.1, may 11th 2011, Lorca earthquake (southeast Spain) is presented and discussed. This interferometric technique, based on real aperture radar (RAR), allows an easy, non-invasive and contactless procedure to evaluate the dynamic response of a building excited by ambient vibration noise. Contemporaneously, a 3D computational model of the monitored structure has been developed and an equivalent non-linear static analysis has been performed. The capacity spectrum method and a specific fragility model were used in order to obtain a global damage index of the structure. A specific post process of the RAR output combined with the numerical analysis of the modelled structure should help to establish the damage condition of the building in the aforementioned specific post-earthquake scenario, in order to estimate the occupancy conditions. The results of the computational assessment are consistent with the observed damage and with the results of the experimental RAR survey. The consistency of the results allows considering the interferometric RAR technique as an interesting alternative, or, in any case, a complementary non-invasive prospecting tool to assess the structural health conditions in a post-earthquake scenario.

Keywords: Ambient vibration; Capacity spectrum; Damage index; Non-invasive; Real aperture radar.

1. INTRODUCTION

The interest in the capability to monitor a mechanical system with the object of detect and characterize damage, at the earliest stage, is prevalent throughout the mechanical, civil, nuclear and aerospace engineering fields (Doebling et al, 1996). In this paper, an original method oriented to the evaluation of the level of damage in structural systems and buildings will be exposed. The basis of the proposed methodology is examining changes in measured ambient vibration response of surveyed buildings by means of a coherent microwave Real-Aperture-Radar (RAR) processed by interferometric techniques.
Ambient vibration testing has become a useful tool for engineers to assess the operational conditions of a structure, allowing maintaining it in a continuous monitoring with the aim of checking the evolution of its health conditions. The monitored kinematic variables allow obtaining complete modal information of the vibrational behaviour of the structure and thus making it possible to infer its operational conditions. The operational conditions of buildings and other structures can be seriously affected after an earthquake impeding, due to obvious security reasons, the inspection inside the constructions and the subsequent evaluation of experts. This makes appropriate the use of alternative non-invasive and contactless means and techniques to safely survey and report about the structural

[1]PhD student, Department of Structural Engineering, UPC, Barcelona, Spain, ecabrerav@uazuay.edu.ec
[2]Professor, Department of Structural Engineering, UPC, Barcelona, Spain, jose.ramon.gonzalez@upc.edu
[3]Researcher, Dept. of Remote Sensing-Division of Geomatics. CTTC. Castelldefels, Spain, guido.luzi@cttc.cat
[4]Researcher, Department of Civil and Environm. Eng., UPC, Barcelona, Spain, yeudy.felipe.vargas@upc.edu
[5] Professor, Department of Civil and Environmental Engineering, UPC, Barcelona, Spain, lluis.pujades@upc.edu

health and the operative conditions of constructions. Consequently, after an extreme event, such as an earthquake, the RAR technology can be used for rapid condition screening, which is intended to provide, in near real-time, reliable information about building performance and its subsequent integrity.

This work describes a damage assessment of an earthquake-damaged building by means of a non-invasive experimental sensing technique and a simulation procedure. An analysis of the building vibrational behaviour is done by applying a monitoring experimental technique complemented by a numerical simulation procedure aiming to assess the building vulnerability and to establish the present operational conditions of the damaged building. The experimental survey measurements, obtained through non-invasive and contactless radar prospecting, describe the actual vibrational and operational behaviour. Additionally, the numerical analysis, performed by an approach of incremental static analyses, describes the path followed by the building through different damage states starting from the null damage state and reaching the present damage state.

The surveyed reinforced concrete building is representative of a group of 15 housing buildings (Figure 1) located in the neighbourhood of San Fernando in the city of Lorca (Murcia, Spain). This building was severely damaged during the Lorca (Murcia, Spain) 2011 earthquake, which with an Mw=5.1 magnitude produced an anomalous high acceleration (PGA~0.37g) in the city causing significant damage. Figure 1.b shows a picture of the assessed building and a detail of damage in one of its column-floor connections corresponding to the first floor. Figure 2.b shows the registered E30N and N30W accelerograms signals and their spectra corresponding to the Lorca (Murcia, Spain) 2011 earthquake. During the experimental radar campaign, and for obvious security reasons, the access to the buildings and the neighbouring area was strictly restricted because the tasks of damage evaluation of the buildings were unfinished. We had an administration permission to measure a single and specific building.

a. **b.**

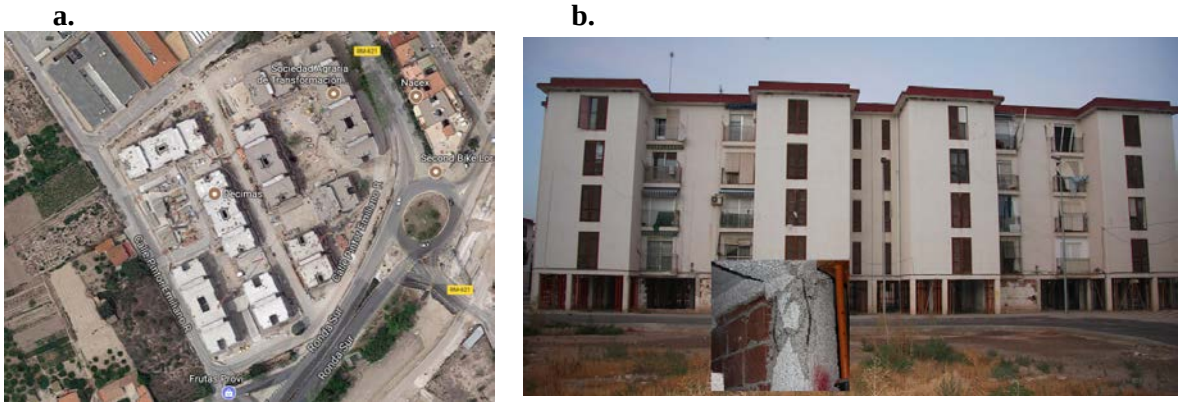

Figure 1. a) An aerial view of the San Fernando Neighbourhood (Source: Google Maps, 2017); b) Front façade of the surveyed building as damaged after the Lorca (Spain) 2011 earthquake and detail of a first floor damaged column. (Source: the authors).

Approximately 72 hours after the earthquake, a first estimation of the occupancy conditions of 7800 buildings in Lorca was completed by onsite inspections performed by 200 experts composed by building construction specialists of the city council and the regional administration with the support of volunteer technicians. The city was divided into a total of 29 sectors where teams composed by two specialists and supported by firemen, specialists of the Spanish Military Unit of Emergency (UME) and foremen, among others, were in charge of the evaluation of building conditions and, if necessary, undertaking emergency tasks to ensure the stability of the buildings. To set up a quick estimation of the occupancy conditions and due to the absence of prior protocols, a simple colour code (Table 1) was defined on the basis of criteria established *ad hoc*. Regarding the studied buildings, the on-site conducted field work exhibited the results shown in Figure 2.

Table 1. Results of the initial prompt inspection (72 hours after the earthquake) of building conditions (From Pascua-Santamaria et al. 2012).

Colour code	Building damage state	Number of buildings	%
Black	Complete	381	4,88
Red	Severe/Extensive	645	8,27
Yellow	Slight to moderate	1502	19,26
Green	Non structural damage	5272	67,59

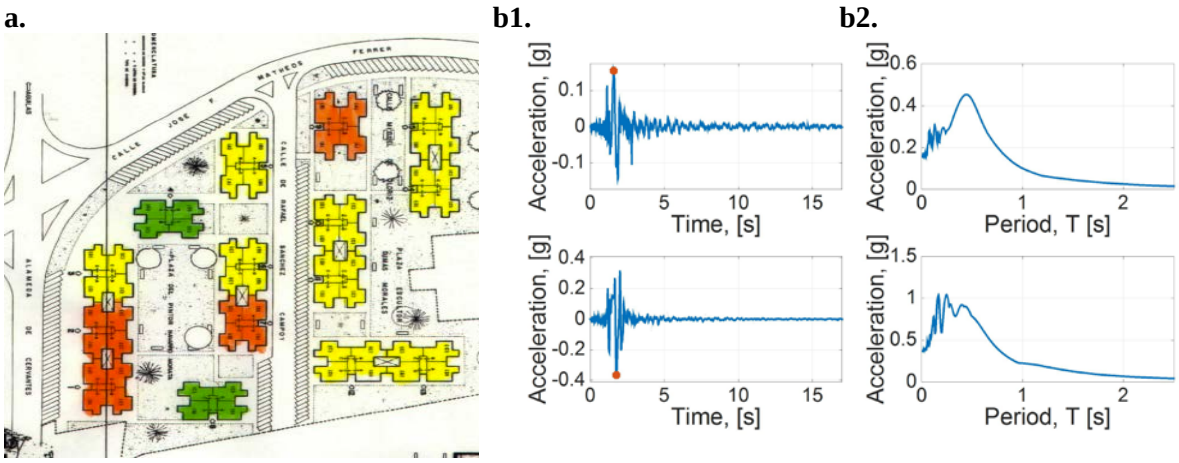

Figure 2. a) Damage distribution in the 15 buildings of San Fernando neighbourhood; b) the Lorca (Spain) 2011 earthquake: b1) Registered E30N and N30W accelerograms signals; b2) Response spectra.

The experimental data, to be compared to the simulation results, have been obtained using a coherent microwave Real-Aperture-Radar (RAR) processed by interferometric techniques. This original contactless technique is able to provide a monitoring of the vibration behaviour of the surveyed building. The use of interferometric radar to evaluate the vibration state of structures as bridges, has been investigated since the nineties (Farrar et al. 1999) and the methodology consolidated in the following decade (Pieraccini et al. 2003; Pieraccini et al. 2005; Gentile and Bernardini 2010), making it also available a commercial system (Coppi et al. 2010). Several papers have been published about the monitoring of bridges (Pieraccini 2006; Gentile and Bernardini 2008; Stabile et al. 2013), wind turbine towers, (Pieraccini et al. 2008), buildings (Luzi et al. 2012; Negulescu et al. 2013) and tall buildings (Luzi et al. 2014) ancient tower (Gentile and Saisi. 2011; Atzeni et al. 2010). In the last years also the development of novel systems has been suggested by different research groups (Grazzini et al. 2009; Cunlong et al. 2015). Among the main advantages of this microwave technique is the capability to measure directly displacements with amplitude down to tens of microns and operating H24 and negligibly affected by weather conditions.

The numerical simulation procedure analyses the development of the building damage, in terms of the evolution of its fundamental period, when the building capacity is compared to the demand represented by the spectrum of the Lorca (Spain) 2011 earthquake. The procedure followed for the capacity and fragility assessment is based on the capacity spectrum method, where the capacity of the structure is compared to the seismic demand (ATC-40 1996). According to the guidelines described in ATC-40, the capacity curves are obtained by means of a pushover analysis. The capacity curves and the demand spectrum are converted to the acceleration-displacement response spectra (ADRS) format (ATC-40 1996). Afterwards, the fragility curves corresponding to the building model are developed. This part of the analysis is performed according to the simplified procedure proposed in the RISK-UE project (2004) (Lagomarsino and Giovinazzi 2006; Barbat et al. 2006; Barbat et al. 2008).

2. DISPLACEMENT MONITORING AND THE RADAR TECHNIQUE

According to the meaning of its acronym, RAdio Detection And Ranging, a radar is able to detect and range objects. The radar acquires echoes from the different targets included in its antenna field of view (FOV): the amplitude peaks located at different distances correspond to contributions from parts of the observed structure. According to the radar equation, the operating distance and the surface characteristics of the backscattering surface strongly affect the radar response. Although the available spatial resolution and the vision of the radar prevent to see details as optical systems do, this methodology allows retrieving simultaneously the displacement vibration history of different parts of the monitored building totally from remote, without the installation of any artificial target. A radar observation uses the time elapsed between the transmission and reception of an electromagnetic waveform to provide a signal, usually called range profile, composed by peaks of different amplitude, which identify the main reflecting parts of the observed structure. Each point of this curve is located at a different distance to the radar, and corresponds to sampling volumes, usually called radar bins. The intersection between these elemental solid unit and the surface of the monitored structure backscattering the transmitted wave, determines the capability to sample unambiguously the monitored structure, as separated elements. The measurement procedure is graphically summarized in Figure 3 and it consists in three main steps. The first is collecting an amplitude profile as a function of the range, sampled at regular spatial steps. Second, when the intensity of the radar echo coming from these elements assures an adequate Signal-to-Noise Ratio (SNR), we can associate to this part of the structure the interferometric phase of the echo; finally a displacement history to analyse is available transforming the phase temporal variations into displacement time signal using the Equation 1.

$$d_{LOS}(t) = \frac{\lambda}{4\pi} \cdot \Delta\varphi(t) \tag{1}$$

Where $\Delta\phi(t)$ is the difference between the phases measured in two successive radar acquisitions, λ the wavelength of the transmitted wave. The scheme depicted in Figure 3 graphically supports the understanding of this geometry resuming the assumed main three steps to apply this methodology.

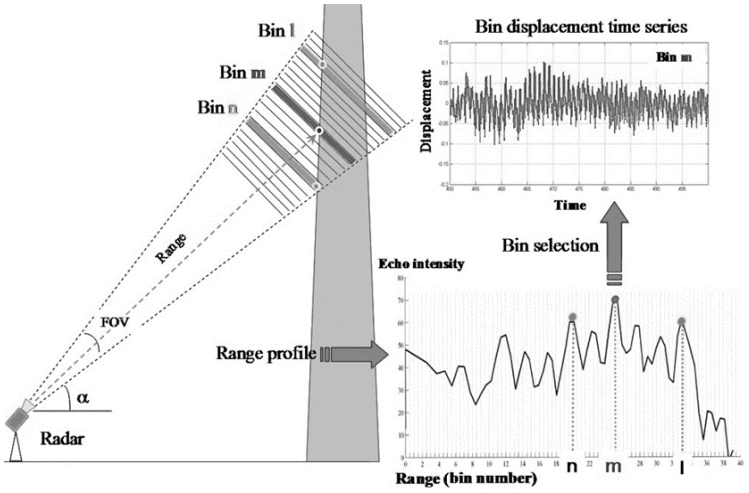

Figure 3. Scheme of the standard procedure aimed at retrieving displacement time series from the radar acquisition. The radar collects an amplitude profile as a function of the range, sampled at regular spatial steps, the radar bins. A displacement time signal is obtained from the interferometric phase of the echo of the selected bin.

The retrieval of the Line of Sight (LOS) displacement from the measured differential phase of the received radar signal is possible because coherent radar provides also the phase value of the reflected signal that allows, through interferometry, evaluating range variation in terms of fraction of wavelength of the propagating radar wave.

The Centre Tecnològic de Telecomunicacions de Catalunya (CTTC) owns a commercial radar with interferometric capability: the IBIS-S manufactured and marketed by IDS (Ingegneria dei Sistemi SpA). The system consists of a sensor module, a control PC and a power supply unit and data processing software. The sensor module transmits an electromagnetic signal at a central frequency of 17.2GHz (Ku band) with a maximum bandwidth of 300MHz, corresponding to a range resolution of 0.5m. The radar instrument is mounted on a tripod equipped with a rotating head to adjust the bearing of the sensor towards the investigated structure. The maximum acquisition rate is 200Hz, depending on the selected maximum range and decreasing as the maximum operating distance increases. Details on the radar equipment can be found in (Coppi et al 2010). The antennas used in this work are two pyramidal horns with a high gain (Gain=23.5dB) to improve the SNR of the radar measurement. The bins that correspond to the highest signal peaks are usually selected to analyse their displacement time series. The sensor unit is managed by a control PC, through a standard USB communication, which is provided with system management software used to configure the acquisition parameters, store the measurement data and show the displacements in real time.

2.1 Data acquisition

The radar system was installed the 14th September 2012 in the San Fernando district of the city of Lorca (Spain). The Radar location, distance to the building and observation angle are selected for the highest SNR and providing a detectable LOS component of the building displacement with respect to the accuracy of the system. The Radar is located 17.1m far from the façade and with an average elevation angle with respect to the horizon of 37º. The displacement of the building is $\Delta S = d_{LOS}/\cos\theta$, where d_{LOS} is the measured displacement and θ the angle between the horizontal displacement direction and the LOS (or equivalently the arctangent of the ratio height of the bin and the distance between the radar position and the building) which depends on the height of the radar bin. Figure 4 shows the acquired range profile, where 7 bins were selected. A higher SNR indicates a better accuracy: only the points with the highest SNR are analysed. The bins corresponding to reflections from the building are those from bin 35 and 43. The time samples of each bin are then processed to estimate the main vibration frequencies under the solicitation of the microtremor/ambient.

a. **b.**

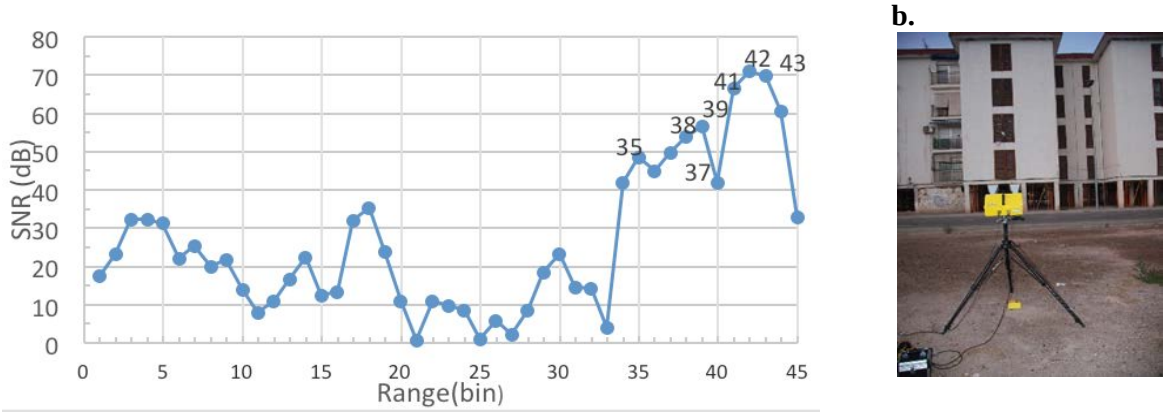

Figure 4. a) Range profile acquired in front of the building. The analysed radar bins are pointed out; b) The RAR equipment measuring the front façade of the building (Source: the authors).

It is worth noting that the radar identifies the different parts of the building with an accuracy of approximately 0.5m in height. In general, the bins with higher SNR perform the better accuracy in measuring the differential phase, but another factor to take into account, in order to evaluate the detection capability of the technique, is the incidence angle of the radar LOS with respect to the vibrating surface. For low incidence angle, the displacement seen by the radar is almost equal to the actual displacement while increasing the angle the fraction of measured displacement decreases. The differential phase samples, are acquired with a 144 Hz sampling frequency, and then band pass filtered (3rd order Butterworth 0.4Hz - 4 Hz) to be transformed in LOS displacement. The filter parameters were selected after calculating the Power Spectral Density (PSD) of the raw samples. The analysis

performed in this work focused on two bins: 35 and 41. The corresponding PSD of these two bins, shown in Figure 5, was calculated by applying the Welch method (Welch 1967). The window used is a Hamming function, the sub-sample duration is 114s and the overlap is 95%. The error in frequency estimation is lower than 0.01Hz.

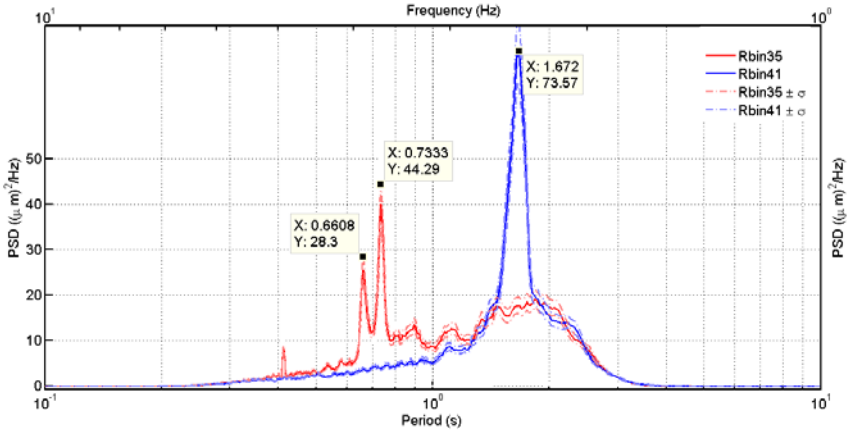

Figure 5. PSD calculated for bin 35 and 41. Two periods outstand from the 35 bin: 0.661 s and 0.733 s while for bin 41 a higher single value is present: 1.67 s.

3. BUILDING AND MODEL DESCRIPTION

The modelled building (Figures 1 and 6) was one of the 15 residential buildings located in the San Fernando neighbourhood of Lorca (Spain). The building, today demolished and substituted by a new construction, had 5 stories and six spans in the studied direction (Figure 6). The design for most buildings was based on a first level diaphanous as a solution in front of severe floods occurred in the region during the 1960-70 decade.

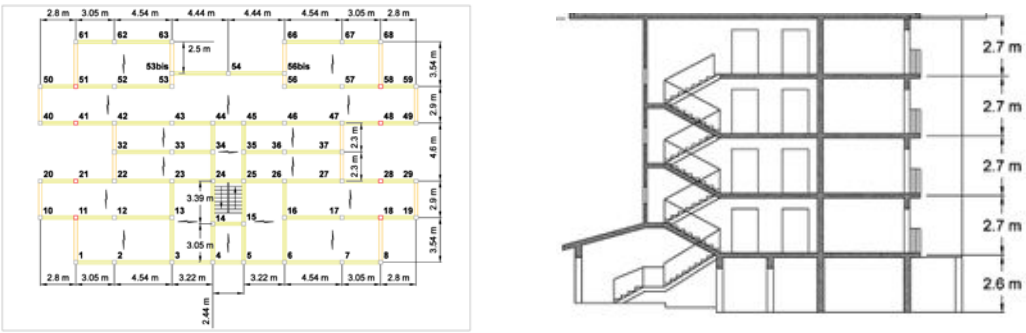

Figure 6. Surveyed building a) Floor plan with the frame distribution and double arrows indicating the orientation of unidirectional slabs b) Cross section of a module.

This soft-storey configuration had influenced the building seismic performance due to the concentration of shear forces and displacements on the weaker frames and induced by an abrupt difference on stiffness in height (Kand and Rawat 2016, Benavent-Climent and Mota-Páez 2017). This is referred to as the common failure mechanism in the damage report of the survey completed after the earthquake (Artés-Carril, 2011). The described damage distribution mainly affected the first level. The few infilled walls present in the entrance (first level) of most buildings collapsed, and the typical infill failure was described as induced by the movement of the surrounding frame. Regarding the columns of the first level, plastic hinges appeared at the bottom and top ends of almost all columns (see detail in Figure 1). Alternatively, a reduced and non-severe distribution of the damage was observed in the upper levels (Artés-Carril 2011).

3.1 Structural description

The surveyed building design was based on a reinforced concrete moment frame structure with unidirectional floors having a thickness of 20cm and closed with infill unreinforced masonry walls. The foundation was conceived by pile caps with ground beams. The longitudinal and transverse reinforcing steel of the frames are very poor and does not observe the reinforcing rules included in contemporary seismic codes. All these elements confirm that the surveyed building was designed without any consideration of the seismic hazard. For concrete a compressive strength f_c=2.06kN/cm^2 is assumed. According to the contemporary codes, the reinforcing steel used at that time was the AE 42N with tensile strength f_y=41.18kN/cm^2. Loads were applied by following the recommendations of Eurocode 8 (EC8 2004).

3.2 Numerical Model

The building has been modelled and analysed by using the SAP2000 software (CSI 2016). Beams and columns were modelled by using a frame type element. The slab is considered to behave as a semi rigid diaphragm and it was modelled by an equivalent linear membrane element with homogeneous thickness. Infilled walls were modelled with a single non-linear membrane element for panels without openings. Geometric non-linearity is also considered by including the P-Delta effect.

4. RESULTS

4.1 Capacity, demand and performance of the building

A modal analysis was performed on the numerical model generated with the SAP2000 software (CSI 2016) which corresponds to the undamaged building (Table 2).

Table 2. Results of numerical modal analysis

Mode	Period (s)	% Mass participation	Axis
Mode 1	0.57	84.1	Horizontal Y
Mode 2	0.57	84	Rotational Z
Mode 3	0.45	73	Horizontal X

The periods measured in the experimental campaign (T_{RAR1}= 0.661s and T_{RAR2}=0.733s) are higher than those calculated from the numerical undamaged model indicating the presence of damage in the existing building. After the experimental campaign, a complete capacity and fragility assessment, based on the capacity spectrum method (ATC-40 1996), is performed on the numerical model. According to the guidelines described in ATC-40, the capacity curve for the analysed building is obtained by means of a pushover analysis (Figure 7). The capacity curve and its corresponding bilinear simplified representation (ATC-40 1996), which is defined by the yielding point [Sd_y, Sa_y] and the ultimate capacity point [Sd_u, Sa_u], are converted to the Acceleration-Displacement Response Spectra (ADRS) format (ATC-40, 1996) as it shown in Figure 7. The main characteristics of the capacity curves are included in Table 3.

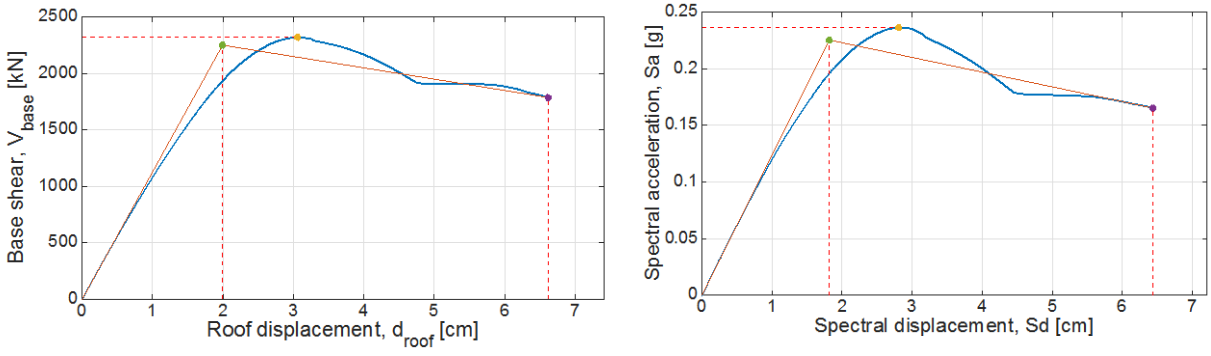

Figure 7. Capacity curve and capacity spectrum and their corresponding bilinear representations for the Y direction.

For the present study, the iterative procedure A, described in the ATC-40 (1996) has been utilized to calculate the performance point of the building (Figure 8.a) taking into account the seismic demand represented in this work by the response spectrum of the Lorca 2011 earthquake (Figure 2.b). Afterwards, the effective period T_{eff}=0.729s, corresponding to the building state reaching the performance point is calculated (Figure 8.b). This calculated effective period is in the range of the experimental periods (T_{RAR1}= 0.661s and T_{RAR2}=0.733s).

Table 3. Main characteristics of the capacity curve and capacity spectrum for the Y direction.

	Capacity curve		**Capacity spectrum**	
	droof (cm)	Vbase (KN)	Sd (cm)	Sa (g)
Yielding point	2.00	2256.16	1.82	0.20
Maximum shear force	3.05	2319.02	2.81	0.24
Ultimate displacement	6.76	1763.46	6.43	0.17

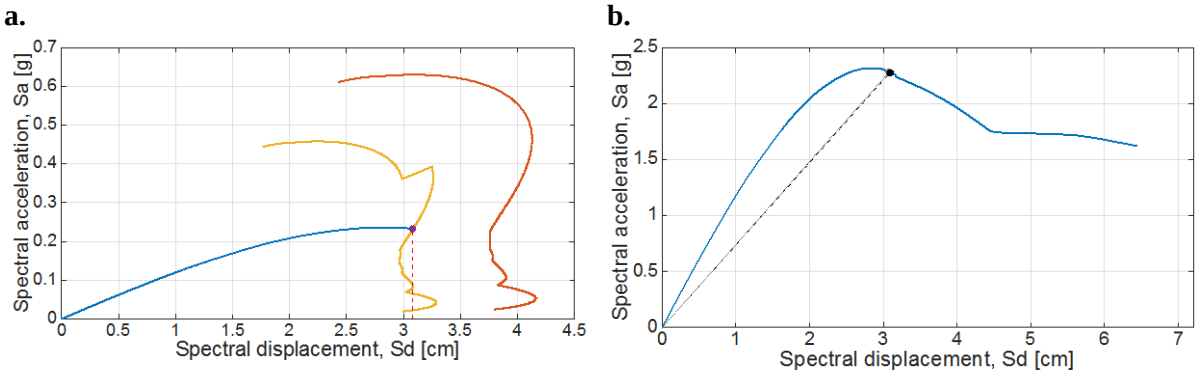

Figure 8. a) Evaluation of the performance point applying the iterative procedure A described in the ATC-40 (1996). b) Determination of the effective period corresponding to the performance point -solid line- and period of the experimental RAR measurement -dashed line-.

4.2 Fragility and damage indices

This part of the analysis is performed according to the simplified procedure proposed in the RISK-UE project (2004). The probability of reaching or exceeding a given state of damage is represented by fragility curves that are described by lognormal cumulative probability functions. The construction of the fragility curves is based on the definition of the yielding point [*Sdy, Say*] and the ultimate capacity point [*Sdu, Sau*] (Lagomarsino and Giovinazzi 2006, Barbat et al. 2006, Barbat et al. 2008). The fragility curves for the modelled building in the +Y direction are shown in Figure 9.a.

The performance point defines the spectral displacement, Sd_p, as the building kinematic response caused by the seismic action. Once this spectral displacement is known, fragility curves allow assessing the probabilities of exceedance of each damage state and, therefore, the probabilities of occurrence of each damage state, or Damage Probability Matrices (DPM), can be easily calculated (Vargas et al. 2013). Additionally, a Damage Index (DI) is defined and used to represent the expected damage by means of a single parameter (Vargas et al. 2013).
Figure 9.b shows the damage function related to the seismic action defined by the response spectrum of the Lorca 2011 earthquake. In this figure a spectral displacement Sd_p=3.2cm corresponding to the performance point is pointed out to illustrate the calculation of DPM and *DI*. Figure 9.c illustrates the corresponding DPM.

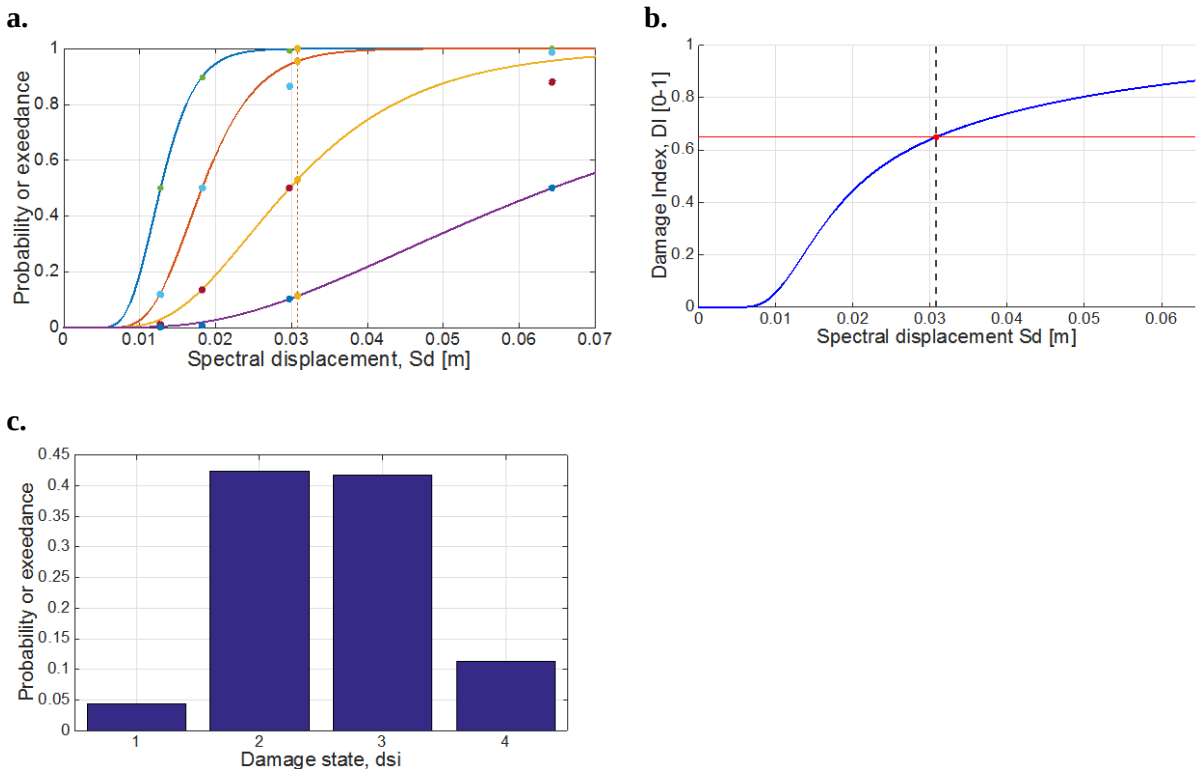

Figure 9. a) Fragility curves for the modelled building in the +Y direction; b) Damage index DI for the Lorca 2011 earthquake; c) Corresponding DPM for the performance point.

4.3 Interstorey drift

A study of the soft storey effect has been performed in this work by means of the analysis of the interstorey drifts. Figure 10 shows the displacements and drift ratios corresponding to each storey of the structure in two different stages: the performance point and the ultimate capacity point. In the performance point stage, the soft floor, which correspond to the first level, get about a 38% of the total displacement and the contribution to the total displacement of higher levels decreases homogeneously to a contribution of the top level of a 7% of the total displacement. Regarding the drift ratio values different construction codes consider that the obtained drift ratio of the first floor corresponds to a mechanism of brittle failure. In the Ultimate capacity point stage, the contribution of the first storey to the total displacement of the structure rises up to 71% and in higher stories it decrease significantly. This evidences that the first storey concentrates almost all the total displacement and, in consequence, all the damage focuses on this first soft storey.

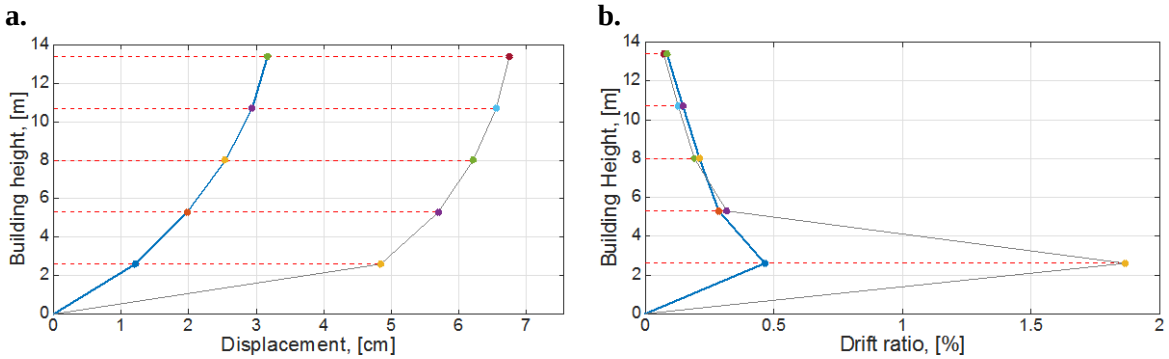

Figure 10. a) Lateral displacement and b) Inter storey drift ratio. Corresponding to two stages: Performance point stage (solid line) and Ultimate capacity stage (dashed line).

5. CONCLUSIONS

The results obtained after combining the ATC-40 (1996) and Risk UE project (2004) procedures include some significant uncertainties in the computed results while the experimental RAR campaign results are exempt of any probabilistic consideration. In any case, in this study the results of the experimental survey, the fundamental periods measured on the damaged building, are in the range of the values obtained by means of the numeric procedures. As described above, the combined numeric procedures ATC-40 (1996) and Risk UE project (2004) include a complete analysis of the variability in the output response due to non-linear effects in the building seismic capacity and in the seismic demand. In consequence, the numerical results represented by the damage probability matrix (DPM) and by the damage index (DI), take into consideration these assumptions and they should be interpreted as a probabilistic approach to the damage state.

The mean damage grade of the whole building represented by the damage index DI=0.64 indicates that the building reached a severe/complete state of damage where the option of reconstruction is not neglected in front of a huge project of retrofitting. An additional interesting observation helps to support the results obtained in this work. The surveyed building and other 14 buildings share the same construction project and all of them are situated in the Lorca neighbourhood. This group of 15 buildings can be considered as a benchmark of the effects of the Lorca (Spain) 2011 earthquake in this specific typology of buildings. The distribution of damage represented by the damage colour code assigned to the group of 15 buildings once affected by the earthquake (Figure 2) is consistent with the obtained damage probability matrix obtained for the studied building typology.

An additional analysis was performed with the purpose of exploring the causes of the severe distribution of damage in this specific building typology. The study of the original construction project details revealed insufficient reinforcing steel in stirrups and longitudinal reinforcements in columns. Additionally, the analysis of the interstorey drift obtained from the non-linear static procedure (pushover analysis) confirmed soft storey behaviour in the first floor due to the abrupt change in the stiffness of the building mainly caused by the absence of inner walls in the first floor. It is straightforward to conclude that the building was designed without any consideration of the seismic hazard and by following construction rules leading to poor reinforcement in concrete elements. Regarding reinforcement rules, present codes are considerably more demanding. In our opinion, all these considerations lead to the development of a weak seismic response.

A main conclusion of this study may be that, for the surveyed building in the San Fernando neighbourhood and after the Lorca (Spain) 2011 earthquake, the results of the experimental RAR campaign are significantly related to the results of the numerical analysis of the building seismic performance in front of the specific demand of the Lorca earthquake. Accordingly, this encourages further research works aiming to explore the possibilities of the RAR technology as a non-invasive and quick prospecting tool oriented to evaluate the damage state of buildings in a post-earthquake scenario.

6. ACKNOWLEDGMENTS AND FUNDINGS

This research has been partially funded by the Ministry of Economy and Competitiveness (*Ministerio de Economía y Competitividad*-MINECO) of the Spanish Government and by the European Regional Development Fund (FEDER) of the European Union (UE) through projects referenced as CGL2011-23621 and CGL2015-65913-P (MINECO/FEDER, UE). Mr. Esteban Cabrera, sponsored by the University of Azuay (UDA), obtained a scholarship from the Ministry of Higher Education, Science and Technology, SENESCYT, Government of Ecuador, for doctoral studies in the Earthquake Engineering program of the UPC-Barcelona Tech.

7. REFERENCES

Artés Carril JM (2011). Estado del grupo de 232 viviendas en Lorca (Barrio San Fernando) tras el terremoto del día 11/05/2011. Technical Report, Instituto de vivienda y suelo, Lorca.

ATC (1996). ATC-40. Seismic evaluation and retrofit of concrete buildings. Applied Technology Council. Redwood City, CA.

Atzeni C., Bicci A, Dei D, Fratini M, Pieraccini M (2010). Remote survey of the leaning tower of Pisa by interferometric sensing. *IEEE GRSL*, (7)1: 185–189.

Barbat AH, Pujades LG and Lantada N (2008). Seismic Damage Evaluation in Urban Areas Using the Capacity Spectrum Method: Application to Barcelona. *Soil Dynamics and Earthquake Engineering*, 28: 851-865.

Barbat AH, Pujades LG and Lantada N (2006). Performance of Buildings under Earthquake in Barcelona, Spain. *Computer-Aided Civil and Infrastructure Engineering*, 21: 573-593.

Benavent-Climent A and Mota-Páez S (2017). Earthquake retrofitting of R/C frames with soft story using hysteretic dampers: Energy-based design method and evaluation. *Engineering Structures*, 137: 19-32.

Coppi F, Gentile C, Ricci PA (2010). Software tool for processing the displacement time series extracted from raw radar data. *Proceedings of the 9th Int. Conference on Vibration Measurements by Laser and non-contact Techniques, Ancona, Italy; 22-25 June 2010. Ed. E.P. Tomasini. AIP Conference Proceeding nr. 1253.*

Cunlong L, Weimin C, Gang L, Rong Y, Hengyi X, Yi Q (2015). A Noncontact FMCW Radar Sensor for Displacement Measurement in Structural Health Monitoring. *Sensors*. 15: 7412-7433.

Doebling SW, Farrar CR, Prime MB, Shevitz DW (1996). Damage Identification and Health Monitoring of Structural and Mechanical Systems from Changes in their Vibration Characteristics: A Literature Review. *Los Alamos National Laboratory report* LA-13070-MS.

Eurocode 8 -EC8- (2004). EN-1998-1. Eurocode 8: Design of structures for earthquake resistance—Part 1. General rules, seismic actions and rules for buildings English version.

Farrar C, Darling TW, Migliorini A, Baker WE (1999). Microwave interferometer for non-contact vibration measurements on large structures. *Mechanical Systems and Signal Processing*. 13(2): 241-253.

Gentile C, Saisi A (2011). Dynamic measurement on historic masonry towers by microwave remote sensing. *Proceeding of the Int. Conf. on Experimental vibration analysis for civil engineering structures*, Vol. II: 524-530. Gentile C and Benedettini F (Eds.), 3-5 October 2011, Varenna, Italy. ISBN978-88-96225-39-4.

Gentile C, Bernardini G (2010). An interferometric radar for non-contact measurement of deflections on civil engineering structures: laboratory and full-scale tests. *Structure and Infrastructure Engineering*, 6(5): 521-534.

Gentile C, Bernardini G (2008). Output-only modal identification of a reinforced concrete bridge from radar-based measurements. *NDT&E International* 41(7): 544-553.

Grazzini G, Pieraccini M, Dei D, Atzeni C (2009). Simple Microwave sensor for remote detection of structural vibration. *Electronics Letters.* Vol. 45 No. 11.

Khan D and Rawat A (2016). Nonlinear Seismic Analysis of Masonry Infill RC Buildings with Eccentric Bracings at Soft Storey Level. *Procedia Engineering*, 161: 9-17.

Lagomarsino S and Giovinazzi S (2006). Macroseismic and mechanical models for the vulnerability and damage assessment of current buildings. *Bull Earthq Eng* 4(4): 415–443.

Luzi G, Crosetto M, Cuevas-González M (2014). A radar-based monitoring of the Collserola Tower (Barcelona, Spain). *Mechanical Systems and Signal Processing*. 49: 234–248.

Luzi G, Monserrat O, Crosetto M (2012). The Potential of Coherent Radar to Support the Monitoring of the Health State of Buildings. *Research in Non-destructive Evaluation.* 23(3): 125-145.

Negulescu C, Luzi G, Crosetto M, Raucoules D, Roullé A, Monfort D, Pujades L, Colas B, Dewez T (2013). Comparison of seismometer and radar measurements for the modal identification of civil engineering structures. *Engineering Structures*. 51: 10–22.

Pascual-Santamaria G, Gonzalez-Lopez S, Alguacil L (2012). Analysis of consequences and Civil Protection activities in the Lorca earthquake (Murcia, Spain): Pre-emergency, Emergency and Post emergency. *Fisica de la Tierra*. 24: 343-362.

Pieraccini M, Luzi G, Mecatti D, Noferini L, Atzeni C (2003). A microwave radar technique for dynamic testing of large structure. *IEEE Transactions on Microwave Theory and Technique*. 51(5): 1603-1609.

Pieraccini M, Fratini M, Parrini F, Pinelli G, Atzeni C (2005). Dynamic Survey of Architectural Heritage by High-Speed Microwave Interferometry. *IEEE GRSL*, 2(1): 28-30.

Pieraccini M, Fratini M, Parrini F, Atzeni C (2006). Dynamic monitoring of bridges using a high-speed coherent radar. *IEEE TGRS*, 11(40): 3284–3288.

Pieraccini M, Parrini F, Fratini M, Atzeni C, Spinelli P (2008). In-service testing of wind turbine towers using a microwave sensor. *Renewable Energy*. (33) 1: 13-21. ISSN: 0960-1481.

Risk-UE project (2004). An advanced approach to earthquake risk scenarios with applications to different European towns Contract number: EVK4-CT-2000-00014. Project of the European Commission.

SAP2000 CSI (2016). Computers and Structures Inc. SAP2000 - Analysis Reference Manual.

Stabile TA, Perrone A, Gallipoli MR, Ditommaso R, Ponzo FC (2013). Dynamic Survey of the Musmeci Bridge by Joint Application of Ground-Based Microwave Radar Interferometry and Ambient Noise Standard Spectral Ratio Techniques. *IEEE GRSL*. 10(4): 870-874.

Vargas YF, Pujades LG, Barbat AH, Hurtado JE (2013). Capacity, fragility and damage in reinforced concrete buildings: a probabilistic approach. *Bull Earthq Eng* 11(3).

Welch PD (1967). The use of fast Fourier transform for the estimation of power spectra: A method based on time averaging over short, modified periodograms. *IEEE Trans. Audio Electroacoust*, AU-15(2): 70-73.